ROYAL SOCIETY OF CHEMISTRY

EDGE ARTICLE

Check for updates

View Article Online
View Journal | View Issue

Triplet dynamic nuclear polarization of pyruvate *via* supramolecular chemistry†

Tomoyuki Hamachi,[a] Koki Nishimura,[a] Keita Sakamoto,[a] Yusuke Kawashima,[a] Hironori Kouno,[a] Shunsuke Sato,[c] Go Watanabe, [cde] Kenichiro Tateishi, [fg] Tomohiro Uesaka[fg] and Nobuhiro Yanai [*abh]

Dynamic nuclear polarization (DNP) significantly improves the sensitivity of magnetic resonance imaging, and its most important medical application is cancer diagnosis *via* hyperpolarized ^{13}C-labeled pyruvate. Unlike cryogenic DNP, triplet-DNP uses photoexcited triplet electrons under mild conditions. However, triplet-DNP of pyruvate has not been observed because of incompatibility of the hydrophobic polarizing agent with hydrophilic pyruvate. This work demonstrates that supramolecular complexation with β-cyclodextrin can disperse 4,4′-(pentacene-6,13-diyl)dibenzoate (NaPDBA), a pentacene derivative with hydrophilic substituents, even in the presence of high sodium pyruvate concentrations. The polarization of photoexcited triplet electron spins in NaPDBA was transferred to the ^{13}C spins of sodium pyruvate *via* triplet-DNP of ^{1}H spins in water and ^{1}H-to-^{13}C cross-polarization. This provides an important step toward the widespread use of ultra-sensitive MRI for cancer diagnosis.

Introduction

Nuclear magnetic resonance (NMR) is an important non-destructive technique for analyzing chemical structures, and magnetic resonance imaging (MRI) is an essential medical procedure. However, both methods are inherently insensitive because the sensitivity is proportional to spin polarization, which is 0.004% for ^{1}H spins and 0.001% for ^{13}C spins under a 6 T magnetic field at room temperature. Hence, MRI is essentially limited to abundant water molecules.

Dynamic nuclear polarization (DNP) improves the sensitivity of NMR[1–10] because it creates a hyperpolarized nuclear spin state by transferring the high polarization of unpaired electron spins.

Dissolution-DNP[11–13] rapidly dissolves hyperpolarized solid samples and has been used for various NMR analyses, such as highly sensitive protein NMR[14,15] and *in vivo* metabolite imaging.[16–20] In particular, [1-^{13}C] pyruvate is the most important probe for high-sensitivity MRI because it is at the center of metabolism and its metabolic kinetics are used in the diagnosis of various diseases, including cancer.[16,17,21–24] Dissolution-DNP has achieved ^{13}C-NMR signal enhancement of more than 10 000-fold;[25] however, it requires severe conditions, such as a high magnetic field (∼7 T) and cryogenic temperatures near 1 K, to use the near-unity electron spin polarization. Alternatively, Overhauser-DNP is a powerful technique that polarizes solutions even at room temperature,[26–29] but the maximum enhancement factor depends on the difference in the gyromagnetic ratio between nuclear spins and electron spins ($\gamma_e/\gamma_H \sim 660$ and $\gamma_e/\gamma_C \sim 2600$).

In contrast, DNP *via* photoexcited triplet electron spins (triplet-DNP) can produce hyperpolarization under milder conditions.[30–34] Photoexcited triplets have large non-equilibrium spin polarizations (∼70% for pentacene[35]) that are independent of temperature, which enables DNP at higher temperatures and lower magnetic fields. Fig. 1A depicts triplet-DNP. After photoexcitation of a polarizing agent, a temporary spin-polarized state is generated by spin-selective intersystem crossing. After the polarization is transferred from the electron spin to ^{1}H spin, it is propagated throughout the solid *via* ^{1}H spin diffusion. Various host molecules and materials have been examined to hyperpolarize drugs,[36–38] water,[39–42] and biologically relevant molecules.[43,44] Dissolution triplet-DNP has been demonstrated.[45,46] However, spin-polarization transfer to lower

^{a}Department of Applied Chemistry, Graduate School of Engineering, Kyushu University, 744 Moto-oka, Nishi-ku, Fukuoka 819-0395, Japan. E-mail: yanai@mail.cstm.kyushu-u.ac.jp

^{b}Center for Molecular Systems (CMS), 744 Moto-oka, Nishi-ku, Fukuoka 819-0395, Japan

^{c}Department of Physics, School of Science, Kitasato University, Sagamihara, Kanagawa 252-0373, Japan

^{d}Kanagawa Institute of Industrial Science and Technology (KISTEC), 705-1 Shimoimaizumi, Ebina, Kanagawa 242-0435, Japan

^{e}Department of Data Science, School of Frontier Engineering, Kitasato University, Sagamihara, Kanagawa, 252-0373, Japan

^{f}Cluster for Pioneering Research, RIKEN, 2-1 Hirosawa, Wako, Saitama 351-0198, Japan

^{g}RIKEN Nishina Center for Accelerator-Based Science, 2-1 Hirosawa, Wako, Saitama 351-0198, Japan

^{h}PRESTO, FOREST, JST, Honcho 4-1-8, Kawaguchi, Saitama 332-0012, Japan

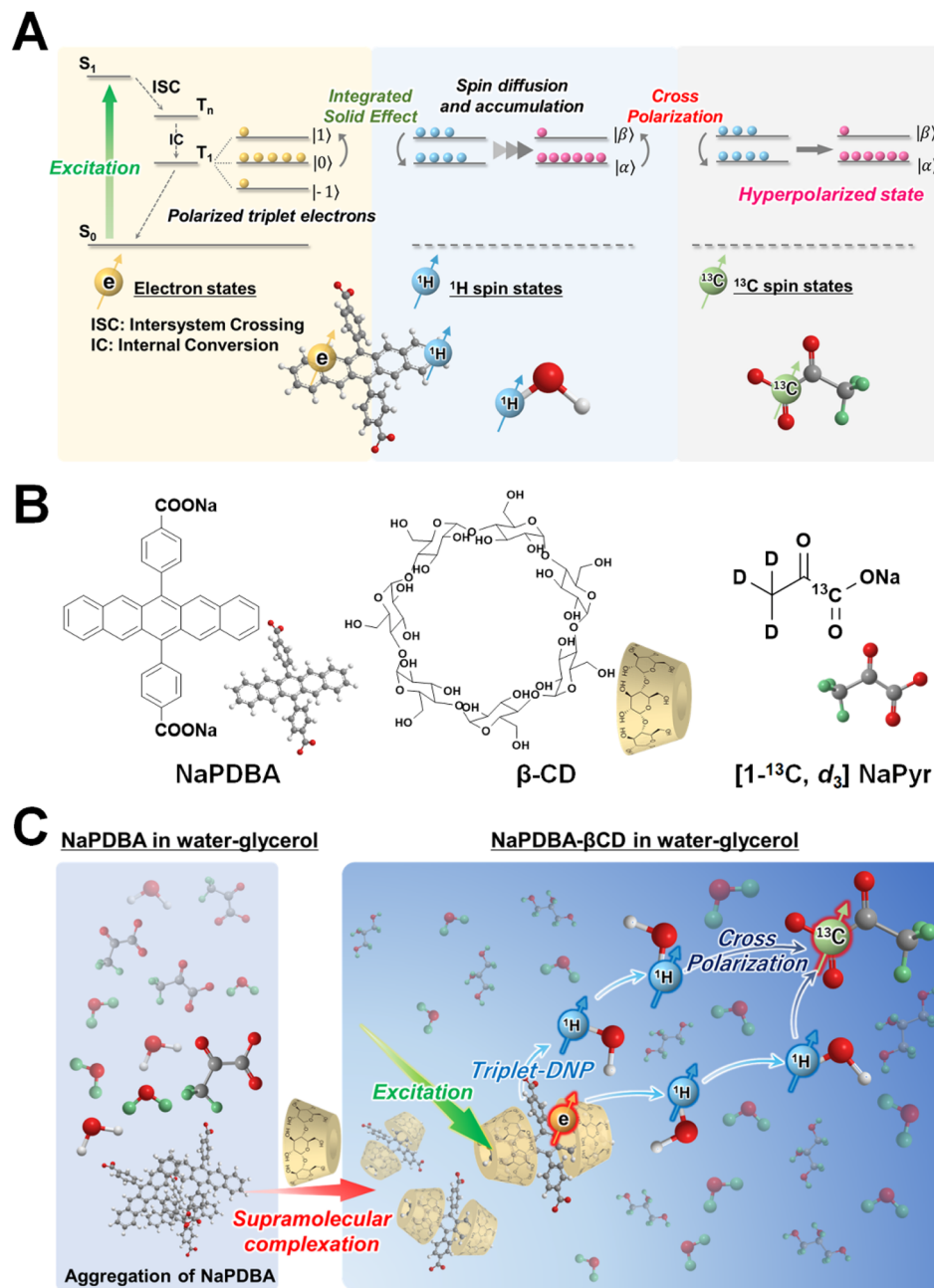† Electronic supplementary information (ESI) available. See DOI: https://doi.org/10.1039/d3sc04123a

Fig. 1 Hyperpolarization of $[1\text{-}^{13}C, d_3]$ sodium pyruvate (NaPyr) by triplet dynamic nuclear polarization (DNP) and cross polarization (CP). (A) Scheme of triplet-DNP and CP. (B) Molecular structures of NaPDBA, βCD, and $[1\text{-}^{13}C, d_3]$ NaPyr. (C) NaPDBA aggregate in DNP juice in the absence of β-cyclodextrin (βCD), but the dispersibility is significantly increased by supramolecular complexation with βCD. Polarization transfer from photoexcited triplet electron spins to ^1H spins of water and then to ^{13}C spins of $[1\text{-}^{13}C, d_3]$ NaPyr.

gyromagnetic ratio spins such as in ^{19}F and ^{13}C *via* cross polarization (CP) has been limited to aromatic molecules,[33,36,37,47] and triplet-DNP of $[1\text{-}^{13}C]$ pyruvate has never been demonstrated because of poor miscibility between the hydrophobic polarizing agent and hydrophilic pyruvate.

Here, we report triplet-DNP of $[1\text{-}^{13}C, d_3]$ sodium pyruvate (NaPyr) at ~100 K and 0.64 T. Higher concentrations of NaPyr are desired for dissolution-DNP application because the polarized spins are diluted after dissolution.[20] Water-soluble polarizing agents were developed and used for triplet-DNP in

aqueous matrices,[41,43,48] but hydrophilic polarizing agents easily aggregate with high concentrations of polar pyruvate. To solve this problem, we used supramolecular chemistry to increase the dispersion of the polarizing agent (Fig. 1B). Cyclodextrin can encapsulate hydrophobic dyes in water,[49,50] and the triplet-DNP of water was observed by using 4,4′-(pentacene-6,13-diyl) dibenzoate (NaPDBA) as a guest in cyclodextrin.[48] NaPDBA aggregation was prevented by supramolecular complexation with β-cyclodextrin (βCD) with a saturated concentration of 1.5 M NaPyr in DNP juice (H_2O/D_2O/glycerol-d_8 = 1/3/6, v/v/v),

a general glass forming solvent.[20] The well-dispersed NaPDBA–βCD complex generated polarization of triplet electron spins, which was transferred to the ¹H spins of water in DNP juice by triplet-DNP and then to the ¹³C spins of [1-¹³C, d_3] NaPyr by CP (Fig. 1C).

Results and discussion

Evaluation of dispersibility of polarizing agents

The dispersed state of NaPDBA in DNP juice was evaluated via absorption spectra (Fig. 2) since random aggregation of polarizing agents could induce rapid relaxation of photoexcited triplet electron-spin polarization, significantly decreasing triplet-DNP efficiency. The π–π* absorption peak of 1 mM dispersed NaPDBA in methanol was observed at 593 nm (Fig. S5†). A red-shift to 604 nm was observed in DNP juice, indicating NaPDBA aggregation (Fig. S6†).[48] When 1.5 M of NaPyr was dissolved in DNP juice, the NaPDBA peak exhibited a large red shift to 614.5 nm, turning the solution blue (Fig. 2). This indicated that the NaPyr salt disrupted NaPDBA hydration and increased its aggregation.[51] The absorption peak was blue-
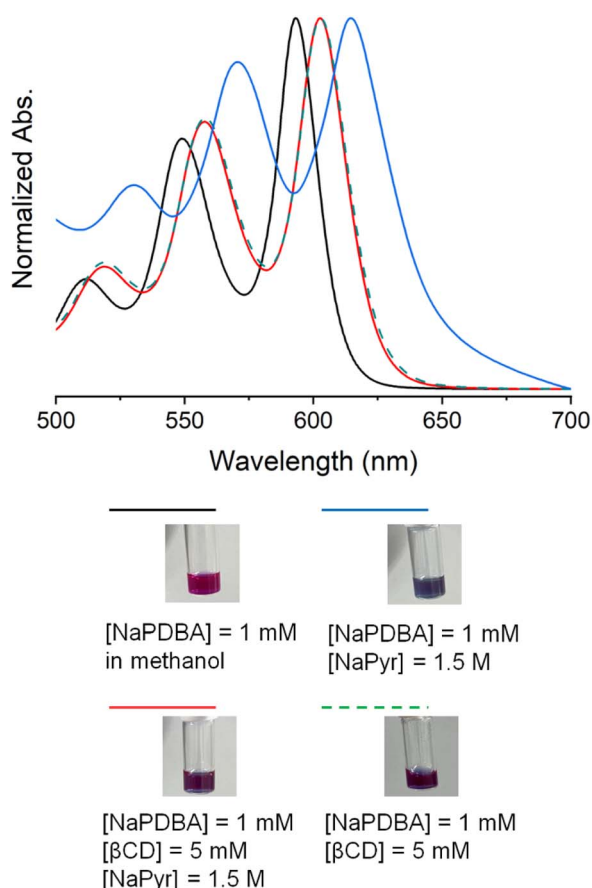

Fig. 2 Dispersion of NaPDBA in the presence of NaPyr. Absorption spectra of NaPDBA in methanol (black line), NaPDBA in DNP juice containing NaPyr (blue line), the NaPDBA–βCD complex in DNP juice (dashed green line) and the NaPDBA–βCD complex in DNP juice containing NaPyr (red line) at room temperature. The concentrations of NaPDBA, NaPyr, and βCD were 1 mM, 1.5 M and 5 mM, respectively. Photographs of each solution are shown.
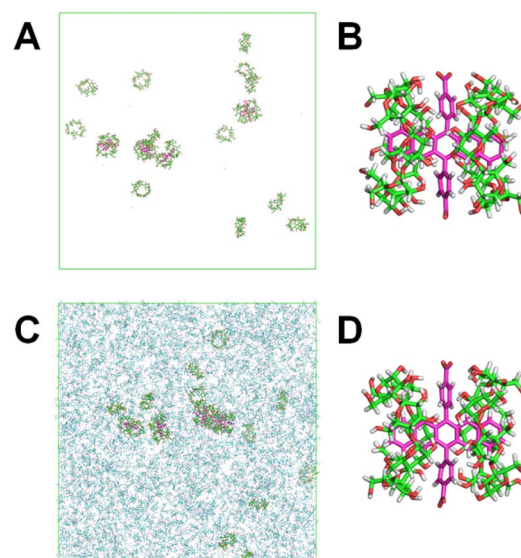
shifted to 603 nm by adding 5 mM of βCD in DNP juice, in the presence of NaPyr (Fig. 2 and S7†). Previously, the 1 : 2 inclusion complex of NaPDBA–βCD was formed in a water–glycerol mixture [glycerol/H₂O (5/5, v/v)],[48] and the absorption peak was also blue-shifted by adding 5 mM of βCD in DNP juice [glycerol/H₂O (6/4, v/v)] in the absence of NaPyr (Fig. S8†). No significant change in the absorption spectra of NaPDBA–βCD in DNP juice was observed with or without NaPyr (Fig. 2). Here, the NaPDBA–βCD inclusion complex was intact at high NaPyr concentrations because the addition of salt increased water structuring and shifted the equilibrium toward the bound state.[52,53]

Evaluation of supramolecular structures

The structure of the NaPDBA–βCD inclusion complex was investigated with NMR and molecular dynamics (MD) simulations. The room-temperature ¹H NMR spectra of NaPDBA shifted upfield when adding βCD in glycerol-d_8/D₂O (6/4, v/v) that contained NaPyr, which indicated formation of the inclusion complex (Fig. S9†).[54,55] Nuclear-Overhauser-effect room-temperature NMR of NaPDBA and βCD in D₂O with NaPyr revealed cross peaks between the NaPDBA pentacene skeleton and the βCD inner region (Fig. S10†). This indicated that NaPDBA was incorporated into the βCD hydrophobic cavity. NMR spectra of NaPDBA and βCD with different concentrations in D₂O which contained NaPyr indicated a 1 : 2 molar ratio of NaPDBA to βCD in the inclusion complex (Fig. S11†). In the MD simulations, the 1 : 2 inclusion complex was stable in glycerol/ H₂O (6/4, v/v) (Fig. 3A and B), and remained stable in the presence of 1.5 M NaPyr (Fig. 3C and D). These results were

Fig. 3 Molecular dynamics (MD) simulations of NaPDBA–βCD supramolecular complexes. (A and B) MD simulation snapshots of the NaPDBA–βCD complex ([NaPDBA] = 1 mM and [βCD] = 5 mM) in glycerol/H₂O (6/4, v/v) at 300 K. Glycerol and H₂O were omitted for clarity. (C and D) MD simulation snapshots of the NaPDBA–βCD complex with NaPyr ([NaPDBA] = 1 mM [βCD] = 5 mM and [NaPyr] = 1.5 M) in glycerol/H₂O (6/4, v/v) at 300 K. Glycerol and H₂O are omitted for clarity.

consistent with the dispersibility of the NaPDBA–βCD complex with and without NaPyr.

Time-resolved ESR measurements

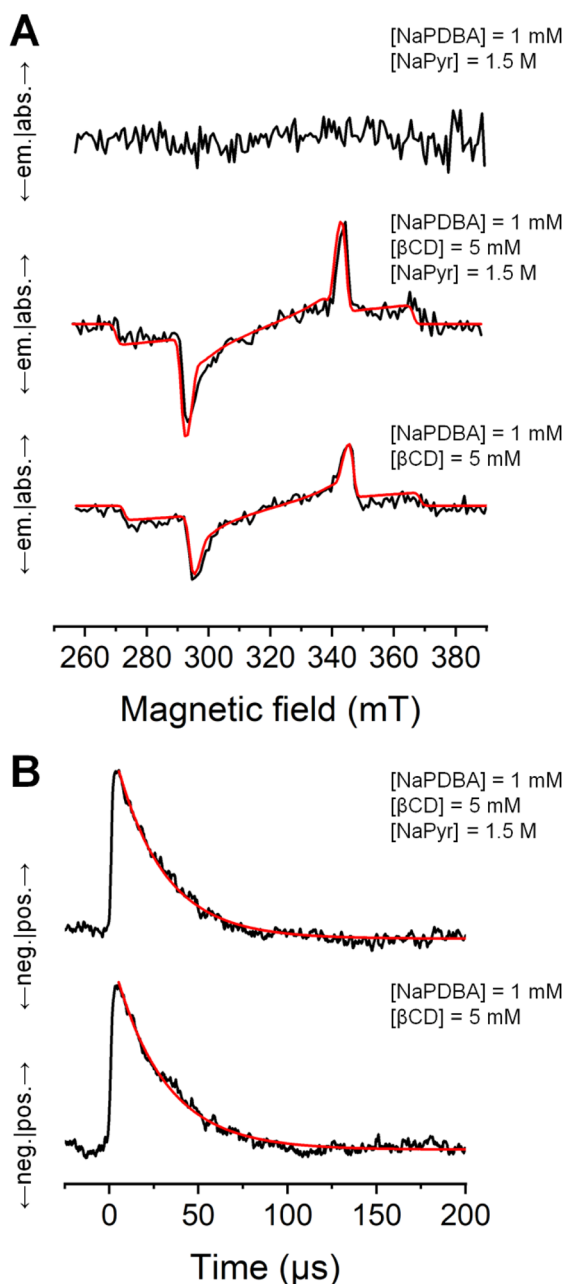The polarization of photoexcited triplet electron spins in NaPDBA in DNP juice was evaluated by time-resolved X-band

Fig. 4 Time-resolved electron spin resonance (ESR) spectra of NaPDBA and peak signal decays in DNP juice (glycerol/H_2O (6/4, v/v)). (A) ESR spectra of NaPDBA containing NaPyr (top), the NaPDBA–βCD complex containing NaPyr (middle), and the NaPDBA–βCD complex (bottom) after 527 nm photoexcitation at 140 K. The concentrations of NaPDBA, NaPyr and βCD were 1 mM, 1.5 M and 5 mM, respectively. Spectra were fitted with the EasySpin toolbox in MATLAB (red lines). (B) Decays of peak ESR signals (black lines). Single-exponential fits are also shown (red lines).

electron spin resonance (ESR) at 140 K (Fig. 4) after 527 nm pulsed-laser excitation. Almost no ESR signal was observed for NaPDBA in DNP juice containing NaPyr in the absence of βCD (Fig. 4A). This was because of random NaPDBA aggregation, which induced rapid relaxation of the triplet electron polarization. When a chromophore aggregate is in a random orientation, the photoexcited triplet electron spins hop between chromophores with different orientations, causing the electron spins subject to magnetic field fluctuations and inducing relaxation of electron spin polarization.[56,57] In contrast, the NaPDBA–βCD complex exhibited a clear ESR signal in DNP juice, even with NaPyr, reflecting well-dispersed NaPDBA via supramolecular complexation. The ESR spectra were fitted with the EasySpin toolbox in MATLAB.[58] The zero-field splitting parameters and relative populations of the NaPDBA–βCD complex were almost the same with and without NaPyr, and were almost the same as those for dispersed pentacene and its derivatives (Table S1†).[59,60] This confirmed that the supramolecular structure was intact in the presence of NaPyr, consistent with the absorption measurements. Fig. 4B shows the signal decay of the ESR absorption peak. The NaPDBA–βCD complex had 27 µs and 29 µs polarization lifetimes in the presence and absence of NaPyr, respectively. These lifetimes were long enough to use the triplet-DNP sequence.

Evaluation of the spin–lattice relaxation time

Because the accumulation of spin polarization via triplet-DNP competes with ^{1}H spin relaxation, a solid sample must have a sufficiently long spin–lattice relaxation time (T_1) for efficient triplet-DNP. The ^{1}H T_1 of glassy DNP juice with NaPDBA and βCD was 46 s at 100 K and 0.64 T, while the addition of NaPyr significantly decreased it to 2 s (Fig. S12†). This was because of increased ^{1}H spin relaxation via methyl group rotation in NaPyr.[61] The use of deuterated sodium pyruvate (d_3-NaPyr) recovered the ^{1}H T_1 (26 s), and the difference from ^{1}H T_1 without NaPyr (46 s) may have been because of remaining ^{1}H spins in the methyl groups of [1-^{13}C, d_3] NaPyr.

DNP measurements

Polarization of the photoexcited NaPDBA triplet electron spins was transferred to the ^{1}H spins of water in DNP juice [glycerol-d_8/D_2O/H_2O, 60/30/10, (v/v/v)] by the ISE sequence at 100 K and 0.64 T (see the ESI for details, Fig. S13†).[31,34] NaPDBA was photoexcited with a 527 nm pulsed laser to produce the polarized electron spins. Then, 17.3 GHz microwaves were irradiated to transfer the polarization from electron spins to ^{1}H spins by matching the frequency of the electron spin in the effective magnetic field in the rotating frame with the Larmor frequency of the ^{1}H spins in the laboratory frame. The magnetic field was swept during microwave irradiation to use more electron spin packets, since the resonant field of the triplet electron spins is broadened by the random orientation of the polarizing agents and hyperfine interactions. By repeating the ISE sequence at 500 Hz, the ^{1}H spins were polarized throughout the glassy DNP juice until the accumulation of ^{1}H spin polarization reaches equilibrium with the spin–lattice relaxation. After the triplet-
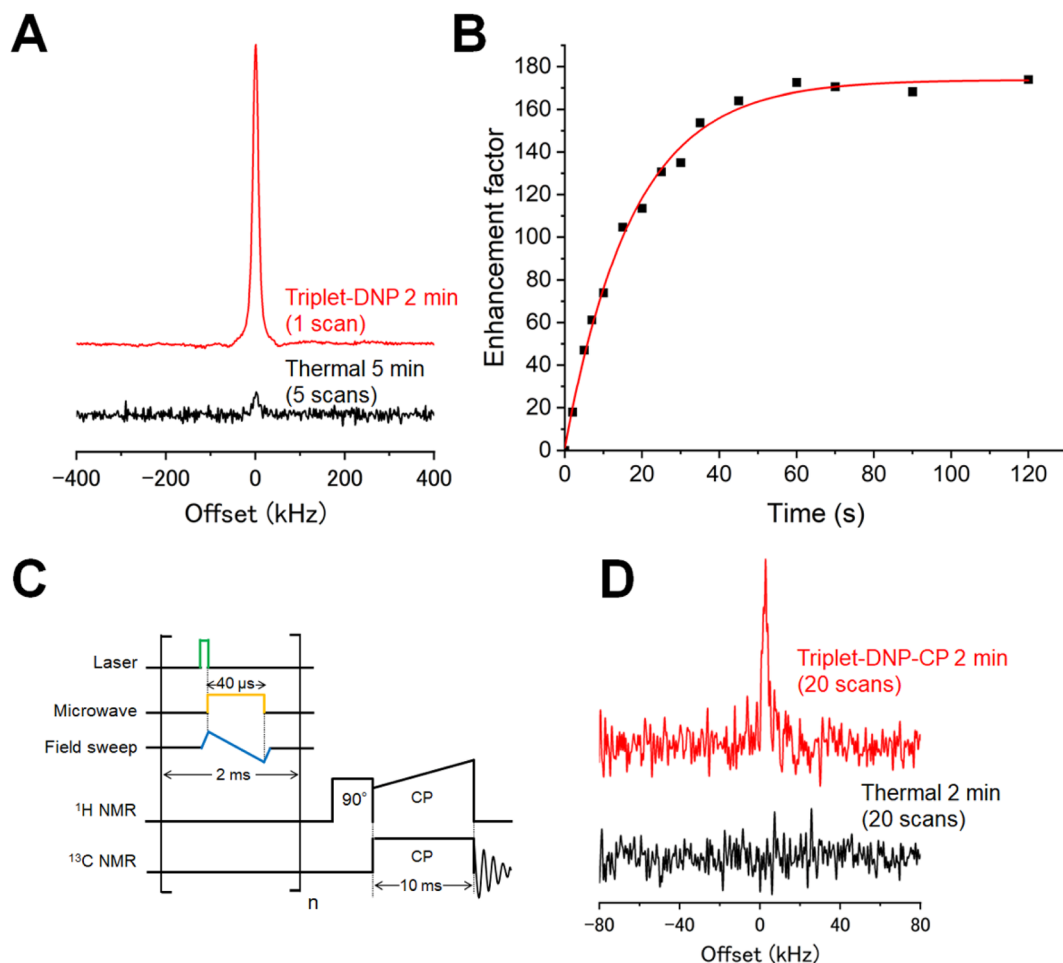
Fig. 5 (A) ^{1}H NMR signals of water in DNP juice (glycerol-d_8/D$_2$O/H$_2$O, 60/30/10, v/v/v) containing NaPDBA, βCD and [1-^{13}C, d_3] NaPyr under thermal conditions (five scans every 5 min) and after triplet-DNP (integrated solid effect sequence for 2 min and 1 scan) at 100 K. (B) ^{1}H polarization buildup curve of DNP juice containing NaPDBA, βCD and [1-^{13}C, d_3] NaPyr at 100 K. The enhancement factors were calculated by comparing the peak areas after triplet-DNP with that of thermal equilibrium. The enhancement factor relative to thermal equilibrium at room temperature is shown. (C) Sequence of triplet-DNP and ramped-amplitude cross-polarization (RAMP-CP). (D) 6.864 MHz ^{13}C NMR spectra of [1-^{13}C, d_3] NaPyr. The red line shows the spectra after triplet-DNP and RAMP-CP (integrated solid effect sequence for 2 min, followed by RAMP-CP, 20 scans) and the black line shows the spectra after RAMP-CP with thermal ^{1}H spins (20 scans).

DNP process in a microwave resonator, the sample was shuttled within 1 s to a coil *via* a motor to acquire ^{1}H NMR. Fig. 5A shows ^{1}H NMR of DNP juice containing 1 mM NaPDBA, 5 mM βCD, and 1.5 M [1-^{13}C, d_3] NaPyr obtained at the thermal state after 2 min of triplet-DNP, in which the accumulation of spin polarization and spin relaxation reached equilibrium. Enhancement factors of 58 and 174 were obtained relative to thermal equilibria at 100 K and room temperature, respectively (Fig. 5B).

The ^{1}H spin polarization in DNP juice was transferred intermolecularly to ^{13}C spins in [1-^{13}C, d_3] NaPyr with a ramped-amplitude cross-polarization (RAMP-CP) sequence (Fig. 5C).[62,63] After triplet-DNP at 100 K and 0.64 T, the sample was shuttled into a double-resonance coil with 27.30 MHz and 6.864 MHz resonance frequencies for ^{1}H and ^{13}C spins, respectively. Polarization transfer from ^{1}H spins to ^{13}C spins was conducted using a 10 ms contact. The irradiated field for the ^{13}C spins was fixed at 20 kHz, while that for the ^{1}H spins was swept over the range of 15–25 kHz. After triplet-DNP and RAMP-CP, enhanced

^{13}C NMR of [1-^{13}C, d_3] NaPyr was observed (Fig. 5D). The enhancement was clear from the fact that no ^{13}C NMR peak was observed *via* RAMP-CP when using ^{1}H spins at thermal equilibrium. ^{13}C-methanol at room temperature was used as a reference, and an enhancement factor of 122 was estimated (Fig. S14†). ^{13}C spins in [1-^{13}C, d_3] NaPyr accounted for ∼85% of the total ^{13}C spins in the entire solid sample; thus, the polarization enhancement factor of the ^{13}C spins in [1-^{13}C, d_3] NaPyr should have been close to 122. Because the theoretical ^{13}C NMR enhancement was ∼4 times (γ_H/γ_C) that of ^{1}H NMR with ideal CP, the CP efficiency was 18%. The low efficiency could be attributed to the absence of ^{1}H spins in [1-^{13}C, d_3] NaPyr, because 40–60% efficiencies were observed when ^{1}H spins were present in the target molecule.[64] Furthermore, ideal CP requires that the radiofrequency pulse amplitude be stronger than the ^{1}H NMR linewidth (∼50 kHz).[65] A higher CP efficiency could be obtained by using a stronger radiofrequency pulse.

Conclusions

In conclusion, triplet-DNP of $[1\text{-}^{13}C, d_3]$ NaPyr, the most important biomolecular probe in MRI applications, was observed by increasing the polarizing agent dispersion *via* supramolecular complexation. It is important to perform DNP with highly concentrated NaPyr, but the method to disperse the polarizing agent in such a highly polar medium had not been clear. Here, the polarizing agent could be modified with ionic carboxylate moieties and then complexed in supramolecular cyclodextrin, which enabled adequate dispersion. This enabled hyperpolarization of the $[1\text{-}^{13}C, d_3]$ NaPyr ^{13}C spins *via* triplet-DNP-CP under a low magnetic field ($\sim$0.64 T) and above liquid nitrogen temperatures ($\sim$100 K). Since the final polarization obtained by triplet-DNP is determined by the build up time constant, T_b, and T_1, higher ^1H and ^{13}C spin polarizations require a shorter T_b and longer T_1. Recently, novel pentacene derivatives showing sharper ESR lines exhibits a shorter T_b than pentacene and the ^1H spin polarization is four times higher than that of pentacene.[66] In addition, the polarization increased 10-fold as T_1 increased from 1 to 3 min, and a spin polarization of 8% was achieved in a model amorphous matrix.[66] Higher ^1H and ^{13}C spin polarization can be obtained by using such a new polarizing agent instead of NaPDBA to obtain shorter T_b and by diluting the ^1H spins or using other matrices with longer T_1. In addition, the implementation of more advanced polarization transfer methods with field/frequency modulation would improve the final spin polarization.[67,68] Hyperpolarized MRI with triplet-DNP will be possible by combining the optimized molecular design of polarizing agents with the key finding of the present study that supramolecular complexation is useful to hyperpolarize NaPyr at high concentrations.

Data availability

All experimental data are available in the article and ESI.†

Author contributions

T. H., Y. K., H. K. and N. Y. designed the research. T. H. and S. K. prepared and characterized the materials. K. T. and T. U. built time-resolved ESR and DNP setups. T. H. and S. K. conducted time-resolved ESR measurements. T. H. and K. N. conducted DNP measurements. S. S. and G. W. carried out MD simulation. T. H., K. N. and N. Y. wrote the manuscript with contributions from all authors.

Conflicts of interest

There are no conflicts to declare.

Acknowledgements

Notes and references

1 T. R. Carver and C. P. Slichter, Polarization of Nuclear Spins in Metals, *Phys. Rev.*, 1953, **92**, 212–213.

2 A. W. Overhauser, Polarization of Nuclei in Metals, *Phys. Rev.*, 1953, **92**, 411–415.

3 D. A. Hall, D. C. Maus, G. J. Gerfen, S. J. Inati, L. R. Becerra, F. W. Dahlquist and R. G. Griffin, Polarization-enhanced NMR spectroscopy of biomolecules in frozen solution, *Science*, 1997, **276**, 930–932.

4 V. S. Bajaj, M. L. Mak-Jurkauskas, M. Belenky, J. Herzfeld and R. G. Griffin, Functional and shunt states of bacteriorhodopsin resolved by 250 GHz dynamic nuclear polarization–enhanced solid-state NMR, *Proc. Natl. Acad. Sci. U. S. A.*, 2009, **106**, 9244–9249.

5 A. Lesage, M. Lelli, D. Gajan, M. A. Caporini, V. Vitzthum, P. Miéville, J. Alauzun, A. Roussey, C. Thieuleux, A. Mehdi, G. Bodenhausen, C. Coperet and L. Emsley, Surface Enhanced NMR Spectroscopy by Dynamic Nuclear Polarization, *J. Am. Chem. Soc.*, 2010, **132**, 15459–15461.

6 J. M. Franck, A. Pavlova, J. A. Scott and S. Han, Quantitative cw Overhauser effect dynamic nuclear polarization for the analysis of local water dynamics, *Prog. Nucl. Magn. Reson. Spectrosc.*, 2013, **74**, 33–56.

7 A. Ajoy, K. Liu, R. Nazaryan, X. Lv, P. R. Zangara, B. Safvati, G. Wang, D. Arnold, G. Li, A. Lin, P. Raghavan, E. Druga, S. Dhomkar, D. Pagliero, J. A. Reimer, D. Suter, C. A. Meriles and A. Pines, Orientation-independent room temperature optical ^{13}C hyperpolarization in powdered diamond, *Sci. Adv.*, 2018, **4**, eaar5492.

8 D. Dai, X. Wang, Y. Liu, X. L. Yang, C. Glaubitz, V. Denysenkov, X. He, T. Prisner and J. Mao, Room-temperature dynamic nuclear polarization enhanced NMR spectroscopy of small biological molecules in water, *Nat. Commun.*, 2021, **12**, 6880.

9 A. Bertarello, P. Berruyer, M. Artelsmair, C. S. Elmore, S. Heydarkhan-Hagvall, M. Schade, E. Chiarparin, S. Schantz and L. Emsley, In-Cell Quantification of Drugs by Magic-Angle Spinning Dynamic Nuclear Polarization NMR, *J. Am. Chem. Soc.*, 2022, **144**, 6734–6741.

10 T. El Daraï, S. F. Cousin, Q. Stern, M. Ceillier, J. Kempf, D. Eshchenko, R. Melzi, M. Schnell, L. Gremillard, A. Bornet, J. Milani, B. Vuichoud, O. Cala, D. Montarnal and S. Jannin, Porous functionalized polymers enable generating and transporting hyperpolarized mixtures of metabolites, *Nat. Commun.*, 2021, **12**, 4695.

11 J. H. Ardenkjaer-Larsen, B. Fridlund, A. Gram, G. Hansson, L. Hansson, M. H. Lerche, R. Servin, M. Thaning and K. Golman, Increase in signal-to-noise ratio of > 10,000 times in liquid-state NMR, *Proc. Natl. Acad. Sci. U. S. A.*, 2003, **100**, 10158–10163.

12 J. H. Ardenkjær-Larsen, On the present and future of dissolution-DNP, *J. Magn. Reson.*, 2016, **264**, 3–12.

13 S. Jannin, J. N. Dumez, P. Giraudeau and D. Kurzbach, Application and methodology of dissolution dynamic nuclear polarization in physical, chemical and biological contexts, *J. Magn. Reson.*, 2019, **305**, 41–50.

14 P. Kadeřávek, F. Ferrage, G. Bodenhausen and D. Kurzbach, High-Resolution NMR of Folded Proteins in Hyperpolarized Physiological Solvents, *Chem.–Eur. J.*, 2018, **24**, 13418–13423.

15 J. Kim, R. Mandal and C. Hilty, Observation of Fast Two-Dimensional NMR Spectra during Protein Folding Using Polarization Transfer from Hyperpolarized Water, *J. Phys. Chem. Lett.*, 2019, **10**, 5463–5467.

16 S. J. Nelson, J. Kurhanewicz, D. B. Vigneron, P. E. Larson, A. L. Harzstark, M. Ferrone, M. van Criekinge, J. W. Chang, R. Bok, I. Park, G. Reed, L. Carvajal, E. J. Small, P. Munster, V. K. Weinberg, J. H. Ardenkjær-Larsen, A. P. Chen, R. E. Hurd, L. I. Odegardstuen, F. J. Robb, J. Tropp and J. A. Murray, Metabolic imaging of patients with prostate cancer using hyperpolarized [1-^{13}C]pyruvate, *Sci. Transl. Med.*, 2013, **5**, 198ra108.

17 K. Golman, R. in 't Zandt and M. Thaning, Real-time metabolic imaging, *Proc. Natl. Acad. Sci. U. S. A.*, 2006, **103**, 11270–11275.

18 F. A. Gallagher, M. I. Kettunen, S. E. Day, D. E. Hu, J. H. Ardenkjær-Larsen, R. Zandt, P. R. Jensen, M. Karlsson, K. Golman, M. H. Lerche and K. M. Brindle, Magnetic resonance imaging of pH *in vivo* using hyperpolarized ^{13}C-labelled bicarbonate, *Nature*, 2008, **453**, 940–943.

19 K. R. Keshari, D. M. Wilson, A. P. Chen, R. Bok, P. E. Larson, S. Hu, M. Van Criekinge, J. M. Macdonald, D. B. Vigneron and J. Kurhanewicz, Hyperpolarized [2-^{13}C]-fructose: a hemiketal DNP substrate for *in vivo* metabolic imaging, *J. Am. Chem. Soc.*, 2009, **131**, 17591–17596.

20 K. R. Keshari and D. M. Wilson, Chemistry and biochemistry of ^{13}C hyperpolarized magnetic resonance using dynamic nuclear polarization, *Chem. Soc. Rev.*, 2014, **43**, 1627–1659.

21 S. E. Day, M. I. Kettunen, F. A. Gallagher, D.-E. Hu, M. Lerche, J. Wolber, K. Golman, J. H. Ardenkjaer-Larsen and K. M. Brindle, Detecting tumor response to treatment using hyperpolarized ^{13}C magnetic resonance imaging and spectroscopy, *Nat. Med.*, 2007, **13**, 1382–1387.

22 A. Z. Lau, A. P. Chen, N. R. Ghugre, V. Ramanan, W. W. Lam, K. A. Connelly, G. A. Wright and C. H. Cunningham, Rapid multislice imaging of hyperpolarized ^{13}C pyruvate and bicarbonate in the heart, *Magn. Reson. Med.*, 2010, **64**, 1323–1331.

23 A. W. Barb, S. K. Hekmatyar, J. N. Glushka and J. H. Prestegard, Probing alanine transaminase catalysis with hyperpolarized ^{13}CD$_3$-pyruvate, *J. Magn. Reson.*, 2013, **228**, 59–65.

24 M. Liu and C. Hilty, Metabolic Measurements of Nonpermeating Compounds in Live Cells Using Hyperpolarized NMR, *Anal. Chem.*, 2018, **90**, 1217–1222.

25 S. Jannin, J.-N. Dumez, P. Giraudeau and D. Kurzbach, Application and methodology of dissolution dynamic nuclear polarization in physical, chemical and biological contexts, *J. Magn. Reson.*, 2019, **305**, 41–50.

26 B. D. Armstrong and S. Han, Overhauser Dynamic Nuclear Polarization To Study Local Water Dynamics, *J. Am. Chem. Soc.*, 2009, **131**, 4641–4647.

27 C. Griesinger, M. Bennati, H. M. Vieth, C. Luchinat, G. Parigi, P. Höfer, F. Engelke, S. J. Glaser, V. Denysenkov and T. F. Prisner, Dynamic nuclear polarization at high magnetic fields in liquids, *Prog. Nucl. Magn. Reson. Spectrosc.*, 2012, **64**, 4–28.

28 J. G. Krummenacker, V. P. Denysenkov, M. Terekhov, L. M. Schreiber and T. F. Prisner, DNP in MRI: an in-bore approach at 1.5T, *J. Magn. Reson.*, 2012, **215**, 94–99.

29 D. Dai, X. Wang, Y. Liu, X.-L. Yang, C. Glaubitz, V. Denysenkov, X. He, T. Prisner and J. Mao, Room-temperature dynamic nuclear polarization enhanced NMR spectroscopy of small biological molecules in water, *Nat. Commun.*, 2021, **12**, 6880.

30 A. Henstra, P. Dirksen and W. T. Wenckebach, Enhanced dynamic nuclear-polarization by the integrated solid effect, *Phys. Lett. A*, 1988, **134**, 134–136.

31 A. Henstra, T.-S. Lin, J. Schmidt and W. T. Wenckebach, High dynamic nuclear polarization at room temperature, *Chem. Phys. Lett.*, 1990, **165**, 6–10.

32 M. Iinuma, Y. Takahashi, I. Shake, M. Oda, A. Masaike, T. Yabuzaki and H. M. Shimizu, Proton polarization with *p*-terphenyl crystal by integrated solid effect on photoexcited triplet state, *J. Magn. Reson.*, 2005, **175**, 235–241.

33 K. Tateishi, M. Negoro, S. Nishida, A. Kagawa, Y. Morita and M. Kitagawa, Room temperature hyperpolarization of nuclear spins in bulk, *Proc. Natl. Acad. Sci. U. S. A.*, 2014, **111**, 7527–7530.

34 K. Nishimura, H. Kouno, Y. Kawashima, K. Orihashi, S. Fujiwara, K. Tateishi, T. Uesaka, N. Kimizuka and N. Yanai, Materials chemistry of triplet dynamic nuclear polarization, *Chem. Commun.*, 2020, **56**, 7217–7232.

35 D. J. Sloop, H. L. Yu, T. S. Lin and S. Weissman, Electron spin echoes of a photoexcited triplet: pentacene in p-terphenyl crystals, *J. Chem. Phys.*, 1981, **75**, 3746–3757.

36 K. Tateishi, M. Negoro, A. Kagawa and M. Kitagawa, Dynamic nuclear polarization with photoexcited triplet electrons in a glassy matrix, *Angew Chem. Int. Ed. Engl.*, 2013, **52**, 13307–13310.

37 S. Fujiwara, N. Matsumoto, K. Nishimura, N. Kimizuka, K. Tateishi, T. Uesaka and N. Yanai, Triplet Dynamic Nuclear Polarization of Guest Molecules through Induced Fit in a Flexible Metal-Organic Framework, *Angew Chem. Int. Ed. Engl.*, 2021, e202115792, DOI: **10.1002/anie.202115792**.

38 S. Fujiwara, M. Hosoyamada, K. Tateishi, T. Uesaka, K. Ideta, N. Kimizuka and N. Yanai, Dynamic Nuclear Polarization of Metal-Organic Frameworks Using Photoexcited Triplet Electrons, *J. Am. Chem. Soc.*, 2018, **140**, 15606–15610.

39 K. Nishimura, H. Kouno, K. Tateishi, T. Uesaka, K. Ideta, N. Kimizuka and N. Yanai, Triplet dynamic nuclear polarization of nanocrystals dispersed in water at room

temperature, *Phys. Chem. Chem. Phys.*, 2019, **21**, 16408–16412.

40 K. Tateishi, M. Negoro, H. Nonaka, A. Kagawa, S. Sando, S. Wada, M. Kitagawa and T. Uesaka, Dynamic nuclear polarization with photo-excited triplet electrons using 6,13-diphenylpentacene, *Phys. Chem. Chem. Phys.*, 2019, **21**, 19737–19741.

41 H. Kouno, K. Orihashi, K. Nishimura, Y. Kawashima, K. Tateishi, T. Uesaka, N. Kimizuka and N. Yanai, Triplet dynamic nuclear polarization of crystalline ice using water-soluble polarizing agents, *Chem. Commun.*, 2020, **56**, 3717–3720.

42 N. Matsumoto, K. Nishimura, N. Kimizuka, Y. Nishiyama, K. Tateishi, T. Uesaka and N. Yanai, Proton Hyperpolarization Relay from Nanocrystals to Liquid Water, *J. Am. Chem. Soc.*, 2022, **144**, 18023–18029.

43 T. Hamachi, K. Nishimura, H. Kouno, Y. Kawashima, K. Tateishi, T. Uesaka, N. Kimizuka and N. Yanai, Porphyrins as Versatile, Aggregation-Tolerant, and Biocompatible Polarizing Agents for Triplet Dynamic Nuclear Polarization of Biomolecules, *J. Phys. Chem. Lett.*, 2021, **12**, 2645–2650.

44 T. R. Eichhorn, A. J. Parker, F. Josten, C. Müller, J. Scheuer, J. M. Steiner, M. Gierse, J. Handwerker, M. Keim, S. Lucas, M. U. Qureshi, A. Marshall, A. Salhov, Y. Quan, J. Binder, K. D. Jahnke, P. Neumann, S. Knecht, J. W. Blanchard, M. B. Plenio, F. Jelezko, L. Emsley, C. C. Vassiliou, P. Hautle and I. Schwartz, Hyperpolarized Solution-State NMR Spectroscopy with Optically Polarized Crystals, *J. Am. Chem. Soc.*, 2022, **144**, 2511–2519.

45 M. Negoro, A. Kagawa, K. Tateishi, Y. Tanaka, T. Yuasa, K. Takahashi and M. Kitagawa, Dissolution Dynamic Nuclear Polarization at Room Temperature Using Photoexcited Triplet Electrons, *J. Phys. Chem. A*, 2018, **122**, 4294–4297.

46 A. Kagawa, K. Miyanishi, N. Ichijo, M. Negoro, Y. Nakamura, H. Enozawa, T. Murata, Y. Morita and M. Kitagawa, High-field NMR with dissolution triplet-DNP, *J. Magn. Reson.*, 2019, **309**, 106623.

47 A. Kagawa, M. Negoro, R. Ohba, N. Ichijo, K. Takamine, Y. Nakamura, T. Murata, Y. Morita and M. Kitagawa, Dynamic nuclear polarization using photoexcited triplet electron spins in eutectic mixtures, *J. Phys. Chem. A*, 2018, **122**, 9670–9675.

48 Y. Kawashima, T. Hamachi, A. Yamauchi, K. Nishimura, Y. Nakashima, S. Fujiwara, N. Kimizuka, T. Ryu, T. Tamura, M. Saigo, K. Onda, S. Sato, Y. Kobori, K. Tateishi, T. Uesaka, G. Watanabe, K. Miyata and N. Yanai, Singlet fission as a polarized spin generator for dynamic nuclear polarization, *Nat. Commun.*, 2023, **14**, 1056.

49 J. Krämer, R. Kang, L. M. Grimm, L. De Cola, P. Picchetti and F. Biedermann, Molecular Probes, Chemosensors, and Nanosensors for Optical Detection of Biorelevant Molecules and Ions in Aqueous Media and Biofluids, *Chem. Rev.*, 2022, **122**, 3459–3636.

50 S. Dutta Choudhury and H. Pal, Supramolecular and suprabiomolecular photochemistry: a perspective overview, *Phys. Chem. Chem. Phys.*, 2020, **22**, 23433–23463.

51 S. Bhattacharya and S. K. Samanta, Unusual salt-induced color modulation through aggregation-induced emission switching of a bis-cationic phenylenedivinylene-based π hydrogelator, *Chem.–Eur. J.*, 2012, **18**, 16632–16641.

52 H. J. Schneider, R. Kramer, S. Simova and U. Schneider, Host-guest chemistry. 14. Solvent and salt effects on binding constants of organic substrates in macrocyclic host compounds. A general equation measuring hydrophobic binding contributions, *J. Am. Chem. Soc.*, 1988, **110**, 6442–6448.

53 R. Holm, C. Schönbeck, P. Somprasirt, P. Westh and H. Mu, A study of salt effects on the complexation between β-cyclodextrins and bile salts based on the Hofmeister series, *J. Inclusion Phenom. Macrocyclic Chem.*, 2014, **80**, 243–251.

54 H.-J. Schneider, F. Hacket, V. Rudiger and H. Ikeda, NMR studies of cyclodextrins and cyclodextrin complexes, *Chem. Rev.*, 1998, **98**, 1755–1785.

55 A. Bernini, O. Spiga, A. Ciutti, M. Scarselli, G. Bottoni, P. Mascagni and N. Niccolai, NMR studies of the inclusion complex between β-cyclodextrin and paroxetine, *Eur. J. Pharm. Sci.*, 2004, **22**, 445–450.

56 W. Bizzaro, L. Yarmus, J. Rosenthal and N. Berk, EPR linewidth of triplet excitons in molecular crystals. II. Tetracene, *Phys. Rev. B*, 1981, **23**, 5673.

57 P. Jaegermann, M. Plato, B. von Maltzan and K. Möbius, Time-resolved EPR study of exciton hopping in porphyrin dimers in their photoexcited triplet state, *Mol. Phys.*, 1993, **78**, 1057–1074.

58 S. Stoll and A. Schweiger, EasySpin, a comprehensive software package for spectral simulation and analysis in EPR, *J. Magn. Reson.*, 2006, **178**, 42–55.

59 M. Schröder, D. Rauber, C. Matt and C. W. Kay, Pentacene in 1,3,5-Tri(1-naphtyl)benzene: A Novel Standard for Transient EPR Spectroscopy at Room Temperature, *Appl. Magn. Reson.*, 2022, **53**, 1043–1052.

60 T.-C. Yang, D. J. Sloop, S. Weissman and T.-S. Lin, Zero-field magnetic resonance of the photo-excited triplet state of pentacene at room temperature, *J. Chem. Phys.*, 2000, **113**, 11194–11201.

61 L. Latanowicz, NMR relaxation study of methyl groups in solids from low to high temperatures, *Concepts Magn. Reson., Part A*, 2005, **27A**, 38–53.

62 G. Metz, X. L. Wu and S. O. Smith, Ramped-Amplitude Cross Polarization in Magic-Angle-Spinning NMR, *J. Magn. Reson., Ser. A*, 1994, **110**, 219–227.

63 A. Pines, M. G. Gibby and J. S. Waugh, Proton-enhanced NMR of dilute spins in solids, *J. Chem. Phys.*, 1973, **59**, 569–590.

64 A. Bornet, R. Melzi, S. Jannin and G. Bodenhausen, Cross Polarization for Dissolution Dynamic Nuclear Polarization Experiments at Readily Accessible Temperatures 1.2 < T < 4.2 K, *Appl. Magn. Reson.*, 2012, **43**, 107–117.

65 A. Bornet, R. Melzi, A. J. Perez Linde, P. Hautle, B. van den Brandt, S. Jannin and G. Bodenhausen, Boosting

Dissolution Dynamic Nuclear Polarization by Cross Polarization, *J. Phys. Chem. Lett.*, 2013, **4**, 111–114.

66 K. Sakamoto, T. Hamachi, K. Miyokawa, K. Tateishi, T. Uesaka, Y. Kurashige and N. Yanai, Polarizing agents beyond pentacene for efficient triplet dynamic nuclear polarization in glass matrices, *Proc. Natl. Acad. Sci. U. S. A.*, 2023, **120**, e2307926120.

67 Y. Quan, J. Steiner, Y. Ouyang, K. O. Tan, W. T. Wenckebach, P. Hautle and R. G. Griffin, Integrated, Stretched, and Adiabatic Solid Effects, *J. Phys. Chem. Lett.*, 2022, **13**, 5751–5757.

68 Y. Quan, M. V. H. Subramanya, Y. Ouyang, M. Mardini, T. Dubroca, S. Hill and R. G. Griffin, Coherent Dynamic Nuclear Polarization using Chirped Pulses, *J. Phys. Chem. Lett.*, 2023, **14**, 4748–4753.